





Article

Influence of Nanoceramic-Plated Waste Carbon Fibers on Alkali-Activated Mortar Performance

Matteo Sambucci ^{1,2,*} , Yazeed A. Al-Noaimat ³ , Seyed Mostafa Nouri ¹ , Mehdi Chougan ³,
Seyed Hamidreza Ghaffar ^{4,5} and Marco Valente ^{1,2} 

¹ Department of Chemical Engineering, Materials, Environment, Sapienza University of Rome, 00184 Rome, Italy; nori.mostafa@gmail.com (S.M.N.); marco.valente@uniroma1.it (M.V.)

² INSTM Reference Laboratory for Engineering of Surface Treatments, UdR Rome, Sapienza University of Rome, 00184 Rome, Italy

³ Department of Civil and Environmental Engineering, Brunel University, London UB8 3PH, UK; yazeed.al-noaimat@brunel.ac.uk (Y.A.A.-N.)

⁴ Department of Civil Engineering, University of Birmingham, Dubai International Academic City, Dubai P.O. Box 341799, United Arab Emirates; s.h.ghaffar@bham.ac.uk

⁵ Applied Science Research Center, Applied Science Private University, Amman 11937, Jordan

* Correspondence: matteo.sambucci@uniroma1.it; Tel.: +39-0644585647

Abstract: Waste carbon fibers as reinforcing elements in construction materials have recently gained increasing interest from researchers, providing outstanding strength performance and a lower environmental footprint compared to virgin fibers. Combination with cement-free binders, namely alkali-activated materials, is becoming increasingly important for sustainable development in the construction industry. This paper presents results relating to the potential use of waste carbon fibers in alkali-activated mortars. The waste carbon fiber fraction utilized in this research is difficult to integrate as reinforcement in ceramic–cementitious matrices due to its agglomerated form and chemical inertness. For this reason, a nanoceramic coating pretreatment based on nanoclay has been implemented to attempt improvements in terms of deagglomeration, dispersibility, and compatibility with alkali-activated materials. After chemical–physical and microstructural analysis on the nanoclay-plated fibers (including X-ray diffraction, IR spectroscopy, contact angle measurements, and electron microscopy) mortars were produced with four different dosages of treated and untreated waste fibers (0.25 wt.%, 0.5 wt.%, 0.75 wt.%, and 1 wt.%). Mechanical tests and fractographic investigations were then performed. The nanoclay coating interacts compatibly with the waste carbon fibers and increases their degree of hydrophilicity to improve their deagglomeration and dispersion. Compared to the samples incorporating as-received fillers, the addition of nanoclay-coated fibers improved the strength behavior of the mortars, recording a maximum increase in flexural strength of 19% for a fiber content of 0.25 wt.%. This formulation is the only one providing an improvement in mechanical behavior compared to unreinforced mortar. Indeed, as the fibrous reinforcement content increases, the effect of the nanoclay is attenuated by mitigating the improvement in mechanical performance.

Keywords: waste carbon fibers; nanoceramic coating; alkali-activated mortars; nanoclay; fiber modification; coating analysis; mechanical performance



Citation: Sambucci, M.; Al-Noaimat, Y.A.; Nouri, S.M.; Chougan, M.; Ghaffar, S.H.; Valente, M. Influence of Nanoceramic-Plated Waste Carbon Fibers on Alkali-Activated Mortar Performance. *Ceramics* **2024**, *7*, 821–839. <https://doi.org/10.3390/ceramics7020054>

Academic Editors: Kamalan Kirubakaran Amirtharaj Mosas and Doni Daniel

Received: 15 May 2024

Revised: 11 June 2024

Accepted: 18 June 2024

Published: 19 June 2024



Copyright: © 2024 by the authors. Licensee MDPI, Basel, Switzerland. This article is an open access article distributed under the terms and conditions of the Creative Commons Attribution (CC BY) license (<https://creativecommons.org/licenses/by/4.0/>).

1. Introduction

The cement industry is responsible for considerable emissions of climate-altering gases every year, accounting for about 7% of the global total carbon footprint [1]. Hence, efforts in developing green alternatives to ordinary cementitious materials are of the utmost importance. Alkali-activated materials (AAMs) are recognized as the most attractive candidates to replace traditional concrete and mortars due to their lower ecological impact, high early strength, excellent corrosion durability, and high-temperature stability [1,2].

Particularly, considering sustainability issues, AAMs are produced from silica and alumina-rich industrial and agricultural by-products (fly ash, slag, silica fume, rice husk ash, palm oil ash), bringing the potential to face challenges of limited available landfill spaces for the disposal of these waste materials [2]. However, just like ordinary cement-based materials, AAMs are brittle, show poor strength to tensile and flexural loadings, and experience sudden failure, limiting their suitability for several structural applications. To address this issue, the inclusion of random short fibers (steel, polymers, carbon, minerals) as reinforcements in AAM composites enhances toughness, ductility, and mechanical strength by bridging and arresting the crack propagation [3].

The implementation of carbon fibers (CFs) as reinforcements for concrete applications provides several benefits in comparison to traditional steel reinforcement. CFs exhibit lower density, higher thermo-mechanical stability, higher strength-to-weight ratio, and most importantly, greater chemical stability and durability [4]. Furthermore, CFs are the most used conductive fillers to realize electrically conductive cement matrices for smart structural health monitoring (self-sensing cementitious composites) [5]. These peculiarities enable the possibility of designing thinner structures without compromising their load-bearing capacity and durability while reducing their environmental impact and making construction more durable, sustainable, and cost-effective [6]. However, the use of virgin fibers is very restricted in the construction materials industry because of their high cost and energy-intensive production process. Indeed, virgin CFs involve higher embodied energies than other synthetic fibers, such as glass fibers, and their utilization is limited in the application fields where the high costs can be justified by a substantial gain in mechanical performance and weight saving (e.g., the aerospace sector) [7].

A “circular” route to strengthen cementitious and alkali-activated concrete or mortars with CFs is the use of recycled fibers. Recycled carbon fibers (rCFs), mainly derived from pyrolysis of CF-reinforced polymeric composites (CFRPs), were recently investigated in the performance of cement-based composites [8–10]. Lamba et al. [8] investigated the influence of the aspect ratio (15 mm and 25 mm fiber length) and volume fraction (from 0.2 vol.% to 1 vol.%) of rCF on the mechanical properties and impact resistance of high-strength concrete mixtures. Experiments revealed that increasing the dosage and aspect ratio of rCFs boosted the flexural and impact strengths of the materials. The results also showed a high level of agreement with the American Concrete Institute (ACI) technical code, enabling the possibility of applications in structural engineering and construction. Patchen et al. [9] studied the addition of short rCFs in ultra-high-performance concrete (UHPC) mixtures, comparing their effect with those of virgin reinforcing fibers in terms of microstructure and mechanical behavior. The authors demonstrated that recycled fibers increased the tensile and compressive strength of UHPC, and their improving effect was comparable to steel fibers and commercially available aerospace-grade CF. Interestingly, rCFs displayed better interfacial bonding with the cement matrix due to the rough surface morphology induced by the recovery processing, resulting in reduced pull-out phenomena. Wang et al. [10] explored the surface modification of rCFs with different chemical treatments (acid, alkaline, and acid–base neutralization) to assess the impact on the mechanical and conductivity properties of cement pastes. With respect to the mixtures incorporating untreated fibers, the surface modification increased the wettability and surface roughness of the rCFs, bringing some improvements in the material’s performance, including an increase in workability (up to 20%), increment in flexural strength (up to 18%), and improvement in electrical conductivity property (up to 40%). Indeed, the treatments remove the residual resin on the fiber surface, increase the roughness, and introduce functional groups to turn rCFs from hydrophobic to hydrophilic.

As discussed, there are several research efforts on the use of rCFs in ordinary cementitious matrices, while the reinforcing effect of these reclaimed fibers in the AAM system is still missing. To the best of the authors’ knowledge, the only contribution comes from Li et al. [11], who investigated the addition of pyrolyzed rCFs in fly ash (FA)–ground granulated blast–furnace slag (GGBS)-based alkali-activated composites. The authors also

implemented an electrochemical oxidation treatment on fibers to improve the compatibility with the matrix. The results revealed that the incorporation of untreated and treated rCFs (1 wt.%) reduced the early-age strength of the composites due to reduced workability and a hindered reaction process. After 28 days of curing, the rCFs improved the flexural strength (+8% with respect to the unreinforced sample). By applying surface oxidation treatment to the fibers, flexural properties were further enhanced due to boosted interfacial adhesion, but this was at the expense of a worsening in compression behavior.

From the survey of the state-of-the-art, two issues requiring further understanding and investigation emerge. Firstly, there is a need to expand knowledge on the functionalization of alkali-activated mortars and concretes using rCFs in the direction of fiber-reinforced composites with augmented performance and eco-friendliness. Secondly, the compatibilization of recycled fibers to enhance the interaction with alkali-activated matrices requires special attention. Regarding the latter aspect, recycled fibers present a fluffy morphology, form bundles, and tend to remain as agglomerates in the binder due to their hydrophobic property and low surface energy. These facts affect their reinforcing ability. Then, treatment after the recycling process of fibers is desired to assist their deagglomeration and good dispersion inside the matrix with the aim of ensuring adequate rheological and mechanical properties [12]. In a previous work [13], the authors developed a surface activation treatment on waste carbon fibers (WCFs) based on nanoclay slurry for integration into cementitious mortars. The fibers stabilized with the nanoceramic coating significantly improved the mechanical performance of the mortars, reporting an increment in flexural strength of more than 75% compared to the plain mixture (no fibers) and exceeding 100% compared to the fiber-reinforced mortar doped with untreated carbon fibers. Furthermore, the proposed treatment did not involve harsh conditions like high temperatures or the use of harmful solvents, resulting in a green method without impairing the economic and ecological benefits of the recycling process.

In the present study, this type of WCF was used for the first time in the production of fiber-reinforced AAM mortars. Considering the successful results achieved with the cementitious systems [13], the simple and non-hazardous surface activation method based on nanoclay was also implemented for alkali-activated matrices to enable full utilization of the WCFs' strength. This work can provide valuable insights into the possibility of using waste fibers in more sustainable cement-free construction materials. The research moves toward achieving sustainable development goals (SDGs) within the construction material industry through the implementation of low-carbon cementitious materials as well as by valorizing clean recycling solutions for composite material wastage.

2. Materials and Methods

2.1. Materials

2.1.1. WCFs

The WCFs involved in this study were provided by the Italian company Carbon Task Srl (Biella, Italy). This fibrous fraction does not come directly from the pyrolysis of post-consumer CFRP parts as in most studies in the literature. WCFs are processing wastes driven by the conversion of scrap CFs (from fabric production) into carbon woven/nonwoven fabrics. This fibrous waste appeared as fluffy carbon agglomerates composed of intertwined fibers of different lengths (Figure 1).

The characteristics of WCFs, experimentally determined in Refs. [13,14], are summarized in Table 1.

Table 1. Properties of WCFs.

Average Fiber Length (μm)	Fiber Diameter (μm)	Agglomerate Density (kg/m^3)
550	6.6	1697



Figure 1. Photograph of WCFs used in this study.

2.1.2. Surface Activation on WCFs

Surface activation on WCFs involved the preparation of a ceramic slurry by dispersing the fiber agglomerates in a nanoclay-based aqueous solution. The attapulgite nanoclay (ANC) used in this work (Figure 2) was purchased from Lawrence Industries Ltd. (Tamworth, UK). The experimental characterization of ANC conducted in previous research [13,14] revealed a bulk density of 7690 kg/m^3 , hydrodynamic diameters from $0.75 \text{ }\mu\text{m}$ to $3.38 \text{ }\mu\text{m}$, and a maximum residue level of 45%.



Figure 2. Photograph of ANC used in this study.

The treatment is comprehensively described in ref. [13] and essentially consisted of mixing WCFs and ANC (at the same weight ratio) in water (Figure 3). The fiber and water dosage used for the slurry was designed to produce the AAM mixtures. First, the required amount of WCFs and water were mixed for 1 min at 500 rpm by means of an overhead stirrer (Ika-Werke GmbH, Staufen, Germany). Then, ANC was added, and stirring at 500 rpm was continued for an additional 30 min. The slurry containing the treated fibers was used as the liquid component in the preparation of the “one-part” AAM samples.

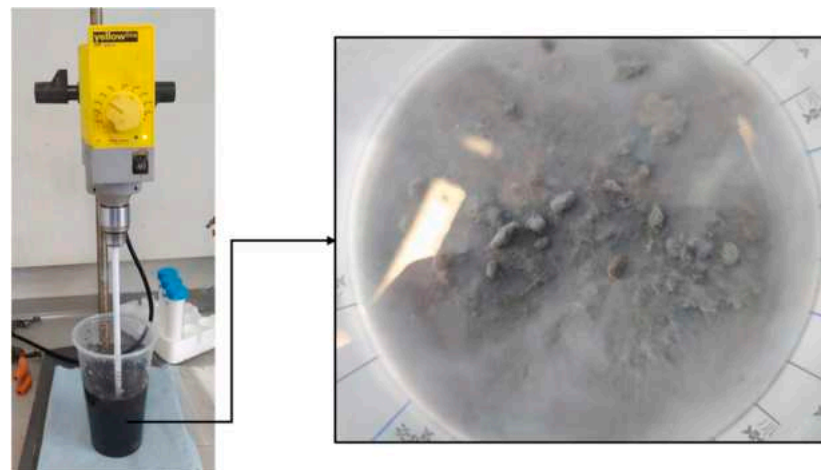


Figure 3. Preparation of WCF-ANC slurry for fiber treatment.

2.1.3. Fiber-Reinforced AAM Composites: Materials, Mix Designs, and Samples Fabrication

Class F-FA, purchased from Cemex UK (Cemex, Coventry, UK), and GGBS, obtained from Hanson UK (Heidelberg Cement Group, Maidenhead, UK), were used as precursors to produce the binary “one-part” alkali-activated mortars. Sodium metasilicate (Na_2SiO_3) in powder form obtained from Fisher Scientific UK (Fisher Scientific, Maidenhead, UK) with a purity of 97.5% and alkalinity modulus ($\text{SiO}_2/\text{Na}_2\text{O}$) of 1.6 was used as the alkali activator. Three types of natural aggregates were employed, including fine river sand (0–0.5 mm), coarse river sand (0.5–1 mm), and quartz sand (0.06–0.3 mm). A detailed characterization of these raw materials has been reported in an author’s previous work [15]. A total of 7 different formulations of alkali-activated mortars were prepared and investigated (Table 2). The control mixture (*WCF0*), without fibers, was used as a basic mix design to realize the fiber-reinforced AAM composites. The mix proportion of the *WCF0* sample consisted of a tailored formulation developed by the authors in past research [15] for integrating waste materials and 3D printing processing. Thus, two sets of fiber-added AAM formulations were produced, considering three additions in weight of WCF (0.5 wt.%, 0.75 wt.%, and 1 wt.%) with respect to the total mass of the precursors (FA+GGBS). The first set, consisting of *WCF0.5*, *WCF0.75*, and *WCF1* mixes, involved adding untreated WCF by simply dispersing the fibers in the required water for 5 min at 500 rpm. The second set, including *WCF0.5-ANC*, *WCF0.75-ANC*, and *WCF1-ANC* mixes, involved the addition of fibers activated with nanoclay-based treatment according to the procedure mentioned in Section 2.1.2.

Table 2. Mix design formulations.

Sample ID	Precursor (kg/m^3)		Aggregate (kg/m^3)			Activator (kg/m^3)	Water (kg/m^3)	Filler (kg/m^3)	
	FA	GGBS	Fine Sand	Coarse Sand	Quartz Sand	Na_2SiO_3		WCF	ANC
<i>WCF0</i>	690	450	700	465	200	135	375	-	-
<i>WCF0.25</i>	690	450	700	465	200	135	375	2.85	-
<i>WCF0.5</i>	690	450	700	465	200	135	375	5.70	-
<i>WCF0.75</i>	690	450	700	465	200	135	375	8.55	-
<i>WCF1</i>	690	450	700	465	200	135	375	11.40	-
<i>WCF0.25-ANC</i>	690	450	700	465	200	135	375	2.85	2.85
<i>WCF0.5-ANC</i>	690	450	700	465	200	135	375	5.70	5.70
<i>WCF0.75-ANC</i>	690	450	700	465	200	135	375	8.55	8.55
<i>WCF1-ANC</i>	690	450	700	465	200	135	375	11.40	11.40

To produce the “one-part” alkali-activated mixtures, all the solid ingredients (FA, GGBS, aggregates, and alkali activator) were dry-mixed for 2 min using a Hobart mixer. Then, tap water (plain, containing crude WCF or containing the fibers treated with ANC) was gradually added to the mixture, and the mixing was continued for a further 10 min. The obtained mixtures were cast in prismatic polystyrene molds ($40 \times 40 \times 160 \text{ mm}^3$), heat cured at $60 \text{ }^\circ\text{C}$ for 24 h, then demolded and kept in a room environment ($20 \pm 3 \text{ }^\circ\text{C}$ and 50% RH) until testing.

2.2. Methods

First, the surface morphology, wettability, and physiochemical characteristics of fibers before and after the nanoceramic surface treatment were characterized by scanning electron microscopy (SEM), X-ray diffractometry (XRD), Fourier transform infrared spectroscopy (FTIR), and water contact angle (WCA) measurements. Then, the treated and untreated WCFs were employed to fabricate “one-part” alkali-activated mortars, investigating the influence of different fiber dosages (0 wt.%, 0.25 wt.%, 0.5 wt.%, 0.75 wt.%, and 1 wt.%). Eventually, the mechanical performance of the AAM composites was experimentally studied regarding the flexural and compressive properties.

2.2.1. Characterization of WCFs after ANC-Based Conditioning

A complete characterization of carbon fibers along the whole process of their conditioning is a prerequisite to understanding the effectiveness of the proposed treatment on the dispersion and, finally, the performance of the produced alkali-activated composites. The effects of ANC-based treatment on the physical and microstructural characteristics of WCF were investigated following different test methods. Samples of carbon fibers treated with nanoclay were obtained by taking a portion of WCF–ANC slurry and oven-drying it on a watch glass at $100 \text{ }^\circ\text{C}$ for 24 h. From the dried material, selected specimens were extracted and subjected to the experimental analysis below (Figure 4).

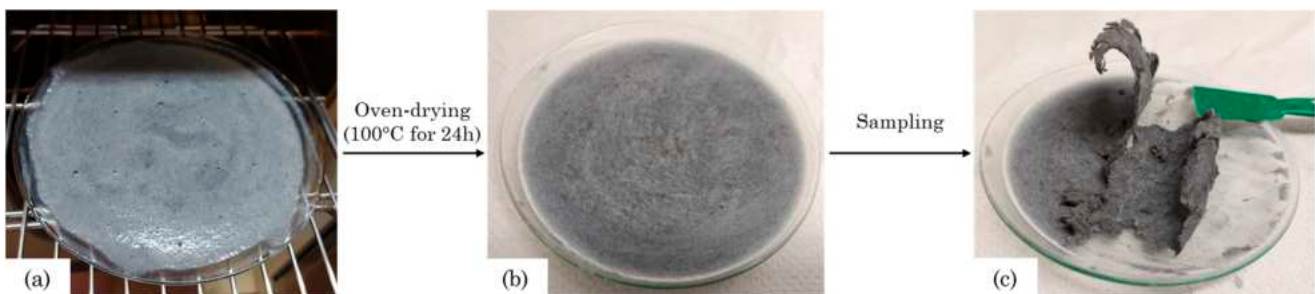


Figure 4. Procedure for obtaining test samples of WCF treated with ANC: (a) placing WCF–ANC slurry on watch glass for drying, (b) oven-dried sample, and (c) sample extraction.

The structural characteristics of as-received WCFs, ANC powder alone, and ANC-treated fibers were studied by XRD using a Philips X’Pert diffractometer (PANalytical BV, Almelo, The Netherlands), operating at 40 KV and 40 mA with $\text{CuK}\alpha 1$ radiation, with a scan range of $10\text{--}90^\circ$ (2θ), feed step of 0.02° , and acquisition time of 2 s.

FTIR spectrometry was implemented to probe the chemical change on the WCF surface induced by the ANC-based conditioning. For this purpose, a PerkinElmer Spectrum 3 FT-IR spectrometer (PerkinElmer, Waltham, MA, USA) was used. For each sample, 4 scans with a resolution of 4 cm^{-1} are taken for spectrum integration in the wavenumber range of 4000 to 400 cm^{-1} .

WCA measurements were performed to compare the wetting behavior of WCF before and after the treatment with ANC. Contact angles on nude and treated fibers were measured at room temperature using an OCA 15 Pro optical analyzer (DataPhysics Instruments, Filderstadt, Germany). The static sessile method was used with ultrapure water as the testing liquid (droplet volume 3 μ L) [16]. WCA values and the droplet spreading at the fiber surface were recorded and analyzed using the SCA 20 image analysis software (DataPhysics Instruments, Filderstadt, Germany) provided with the instrument.

The fiber's microstructure was investigated by SEM analysis. Secondary electron (SE) micrographs were acquired using a Tescan MIRA 3 FEG-SEM (Tescan, Brno, Czech Republic) at an operating voltage of 15 kV. Energy-dispersive X-ray spectroscopy (EDS) analysis was also conducted on these samples using an Edax Octane Elect EDS system detector (Edax, Mahwah, NJ, USA).

2.2.2. Test Methods for Fiber-Reinforced AAM Composites

After the curing time of 7 days, the flexural and compression strength of each AAM formulation were evaluated following the testing standard BS EN 196-1:2016 [17]. An Instron 5960 Series Universal Testing System (Instron, Pianezza, Italy) was utilized for conducting these tests. For the flexural test, the specimens of size 160 \times 40 \times 40 mm, three for each formulation, were subjected to a three-point configuration with a span length of 100 mm. The average values of flexural strength were computed based on the results obtained from these three specimens. After the flexural test, the remaining parts of the tested specimens were subjected to compression tests. The values of compression strength reported are the averages obtained from the results of these four specimens. A loading rate of 1 mm/min was selected for both mechanical tests.

Fractography analysis of the alkali-activated mortars was conducted using SEM (Supra 35VP, Carl Zeiss, Oberkochen, Germany). The inspection was performed on fractured pieces collected for mortar prisms after mechanical testing. Prior to the analysis, the samples were gold coated using an Edwards S150B (Edwards Ltd., Burgess Hill, UK) sputter coater to prevent surface charging effects. SE images of the surface were acquired at an accelerating voltage of 7 kV to ensure meaningful observation.

3. Results

3.1. Characterization of WCFs after ANC-Based Conditioning

3.1.1. Influence of Nanoceramic-Plating on Crystallite Structure of WCFs

The changes in the crystallite structure of WCF following the conditioning with ANC were examined using XRD. The X-ray diffractogram of as-received fibers (Figure 5a) displays two main peaks at around 25° and 45°, which are attributed to (002) and (100) reflections of the stacking of the graphitic planes, respectively [18]. The mineral composition of ANC (Figure 5b) comprises attapulgite, quartz, and montmorillonite. These peaks appear at the same angular position as those detected by other researchers [19]. Figure 5c confirms the presence of nanoclay on the WCF surface. Indeed, the crystalline peaks of the nanoclay associated with quartz and attapulgite overlap the broad graphitic band of carbon fibers (~25°). Furthermore, the patterns reveal all the peaks found in ANC, demonstrating that an effective nanoceramic deposition on the fiber surface occurred. However, the evidence that the carbon-related peaks remain after the nanoclay-based treatment suggests a predominantly physical interaction between the fiber and the ceramic coating which will also be confirmed by the FT-IR analysis below.

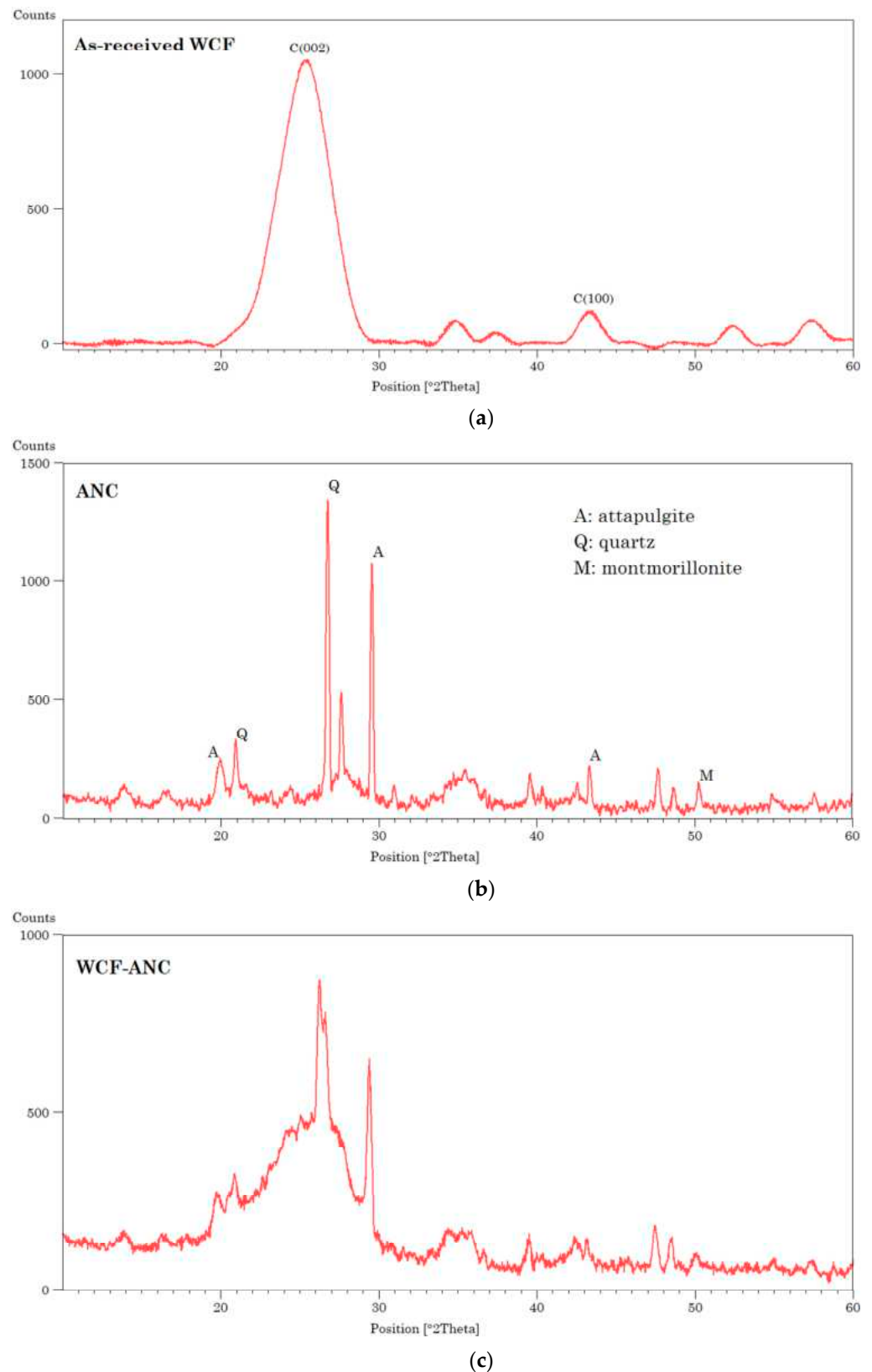


Figure 5. XRD pattern of (a) as-received WCF, (b) ANC, and (c) WCF after treatment with ANC.

3.1.2. Influence of Nanoceramic-Plating on Surface Chemistry of WCFs

The FTIR analysis (Figure 6) again proves the ANC successfully coated the surface of WCF. The ANC spectrum (orange line) shows four main absorption regions. The band

around $3500\text{--}3700\text{ cm}^{-1}$ can be assigned to the stretching of O–H coordinated with metal species (Al, Mg) within the clay structure. The absorption at $\sim 1650\text{ cm}^{-1}$ is correlated with the O–H bending vibration peak of the adsorbed water. The band around 1200 cm^{-1} is ascribed to the Si–O stretching vibration. The absorption region below 500 cm^{-1} results from combined vibrations of Mg–O stretching and O–Si–O and Al–O–Si bending [13,20]. The FTIR spectrum of WCF after conditioning with ANC (black line) highlights the same peak distribution, and no shift of the absorption bands compared to nanoclay alone is detected. Then, ANC-based coating has adequately covered the fiber surface after the treatment. The absence of shifts in the FTIR spectrum confirms that the bond between fiber and nanoclay is based on a physical interaction based on Van der Waals interactive forces and other dispersive interactions. Furthermore, the surface roughness of the fibers would promote the mechanical interlocking of the nanoceramic coating on the WCFs [13].

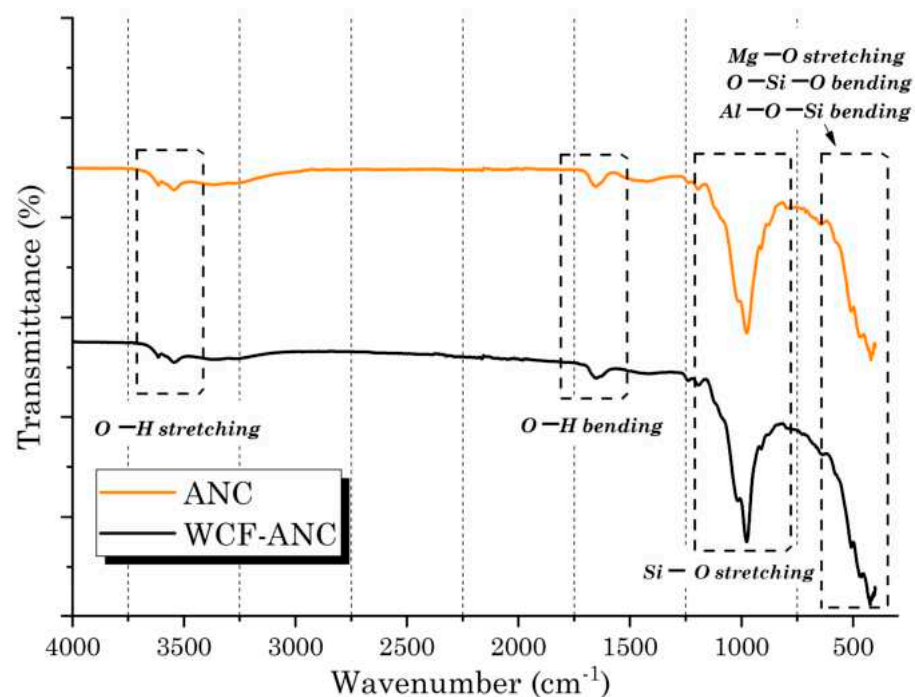


Figure 6. FTIR analysis of ANC and WCF after treatment with ANC.

3.1.3. Influence of Nanoceramic-Plating on Surface Hydrophilicity of WCFs

The effectiveness of fibers for enhancing the structural performance of cement-based materials or AAM is strongly affected by the degree of fiber dispersion. The poor dispersion of fibers into the cement paste results in a weak strengthening action. Deagglomeration and dispersion of the fibers can be attained by improving their hydrophilicity, as the cement or AAM pastes are water-based. The hydrophilic characteristics of fiber can be modified by specific surface treatment before incorporation into the mixture [21]. In addition, increasing the fiber hydrophilicity, which means a low WCA value ($<90^\circ$), helps the establishment of a strong interface cohesion with the matrix resulting in a beneficial influence of the reinforcing agent in terms of mechanical properties and durability [22]. Diblíková et al. [23] implemented a plasma treatment at different argon atmospheres to improve the wettability of CF with the AAM matrix. The results showed that the contact angle reduced from $>90^\circ$ (untreated fibers) to 35° after the plasma treatment and a subsequent positive effect in terms of CF/geopolymer interfacial strength measured by an interlaminar shear strength (ILSS) test. Zhang et al. [24] addressed the challenge related to the agglomeration and poor dispersion of carbon nanofibers in the AAM matrix by using polymer surfactant agents to chemically modify the fiber surface, reducing the surface tension of the dispersion, and preventing aggregation phenomena. Dispersed CF improved the strength of the

resulting AAM composite and refined the material's pore structure, reducing the porosity and pore size.

The hydrophilicity of ANC combined with its cost-effectiveness and environmental compliance were exploited to favorably modify the surface tension of the CFs and facilitate their deagglomeration and dispersion in the AAM matrix. The clay nanoparticles' adhesion onto WCFs led to a significant increase in the water wettability. As expected, the bare WCF showed marked hydrophobicity (Figure 7a), accounting for a WCA value of 138° (average value of 10 measurements). The effectiveness of the surface activation of the fibers with nanoclay is illustrated in Figure 7b. Prior to the complete absorption of the water drop (at 30 ms), a contact angle of about 30° was measured. Then, the water drop was instantly absorbed by the treated fiber bundle after deposition (50 ms), resulting in a complete hydrophilization of the surface that enhances the water affinity and the fiber declustering. A similar method was studied by Lindstrom et al. [25], who investigated the effect of nanoclay surface plating on cellulosic fibers to avoid floc formation and interfiber bonding and give better compatibility with the surrounding matrix.

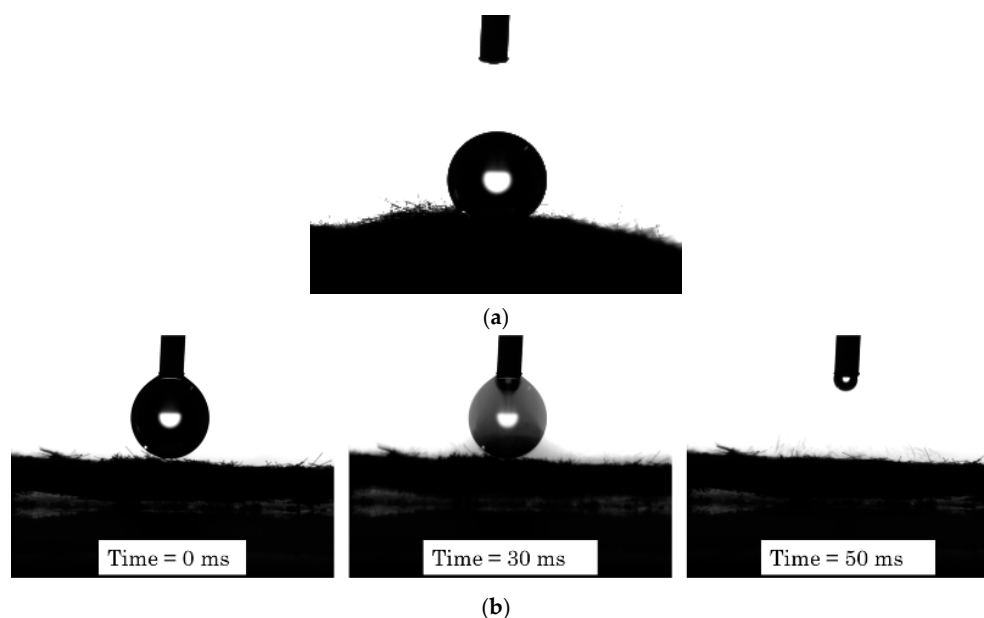


Figure 7. WCA profile for (a) bare WCF and (b) WCF treated with ANC.

3.1.4. Influence of Nanoceramic-Plating on Microstructure of WCF

The morphology of the ANC deposit was examined with the aid of the SEM technique and such observations were performed directly on the fiber surface after the nanoclay-based conditioning and drying of WCF bundles. From Figure 8, the first noticeable feature is the uniform nanoceramic coating along the entire length of the fibers, showing the typical needle-like morphology of ANC [26]. The fibers also exhibit a large number of longitudinal grooves indicative of partial oxidation on the fiber surface resulting from the pyrolysis treatment. It is presumable that the roughest texture of WCF facilitates the physical grafting of the nanoclay particles on the fiber surface [27]. Furthermore, as previously mentioned, such efficient adhesion is also based on van der Waals and other dispersion interactions between nanoclay particles and the WCFs' surface.

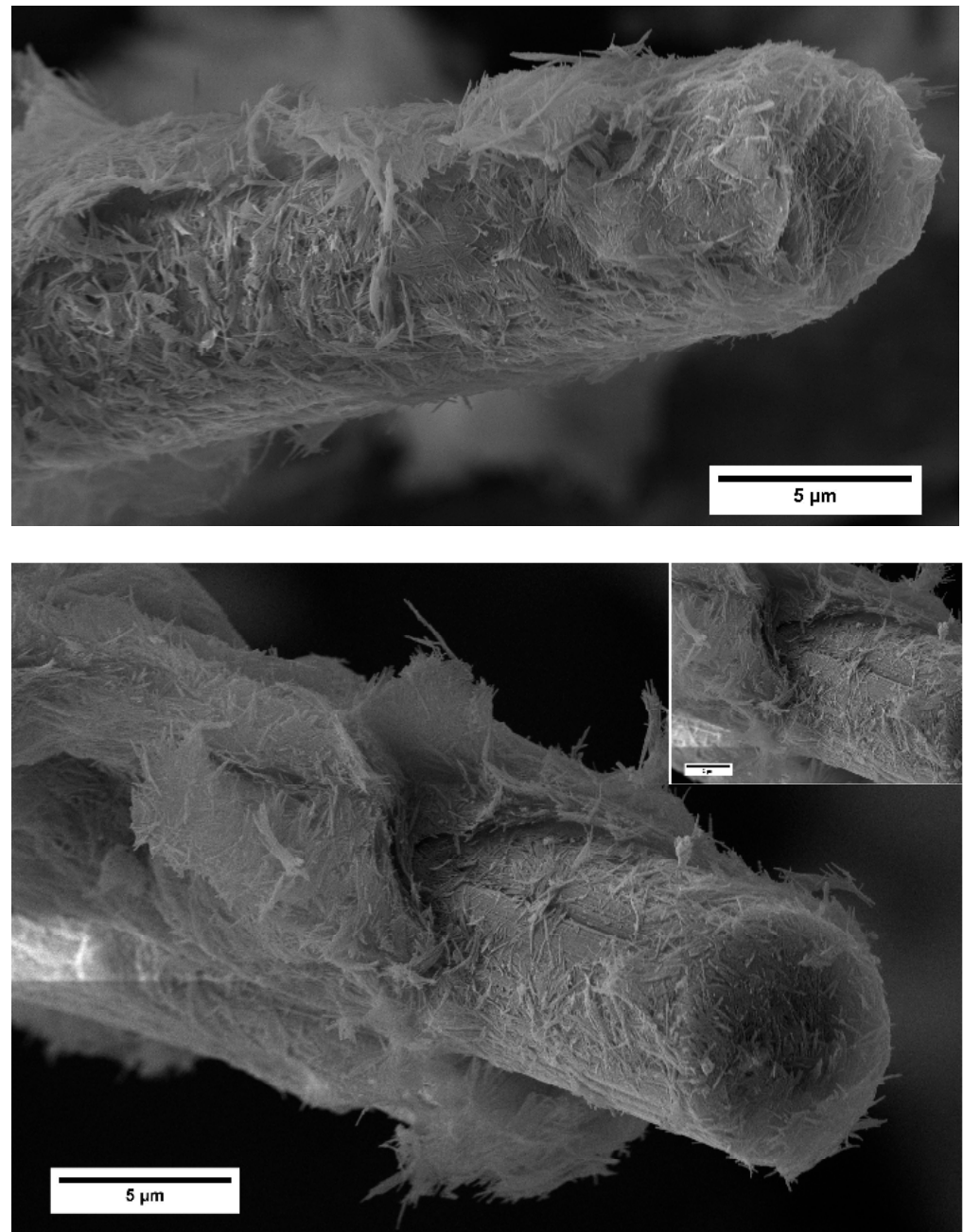


Figure 8. SEM micrographs of WCF coated with ANC.

EDS element analysis (Figure 9) confirms the presence of ANC on the fiber surface. The spectrum comprises Silicon (Si), Magnesium (Mg), Aluminum (Al), and Oxygen (O) referring to the crystalline phases of nanoclay, i.e., quartz (SiO_2), montmorillonite ($[\text{OH}]_4\text{Si}_8\text{Al}_4\text{O}_{20} \cdot n\text{H}_2\text{O}$), and attapulgite ($[\text{Mg,Al}]_2\text{Si}_4\text{O}_{10}(\text{OH}) \cdot 4[\text{H}_2\text{O}]$). The analysis also highlights the absence of Calcium (Ca), one of the elements present in nanoclay [13]. This occurs because after deposition the carbon (C) signal deriving from the fiber predominated and overlaid that of Ca (the emission peaks are energetically very close) and therefore the Ca-signal is no longer discriminable in the spectrum.

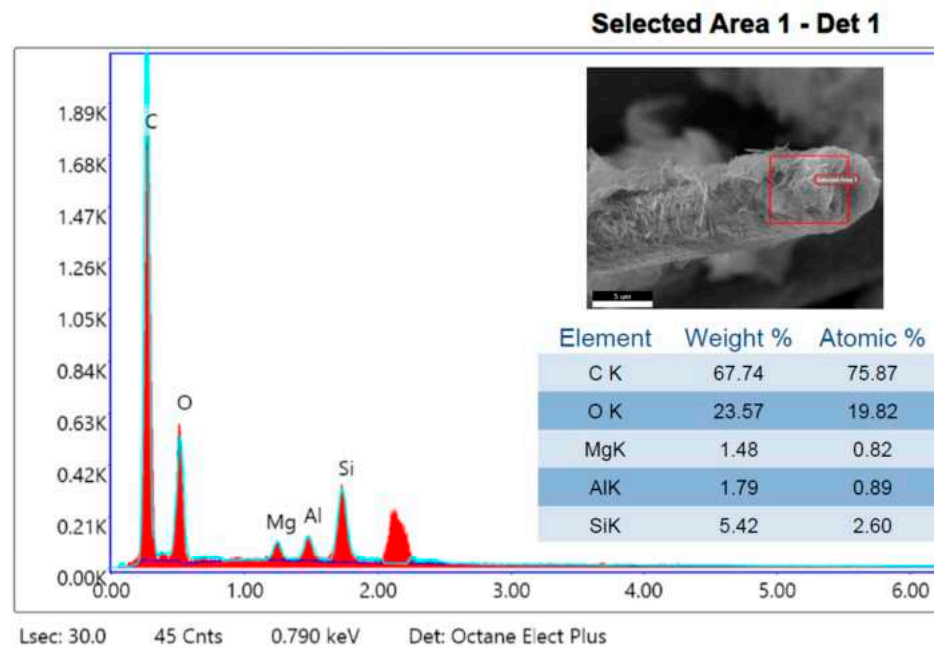


Figure 9. EDS element analysis of WCF coated with ANC.

3.2. Characterization of Fiber-Reinforced AAM Composites

3.2.1. Flexural and Compression Mechanical Testing

Figure 10 displays the flexural test results of alkali-activated mortars reinforced with WCF. The addition of untreated WCF (red plot) induces a worsening effect on the flexural strength which progressively reduces as the fiber content increases. Compared to the control AAM (*WCF0* sample), a decrease from 14% (*WCF0.25* sample) up to 22% (*WCF1* sample) has been detected. The primary reason for this detrimental effect can be ascribed to the lack of adequate deagglomeration of the WCF clusters and, consequently, poor dispersion of the reinforcing fibers in the matrix. Indeed, for achieving an improved contribution in terms of strength performance, a homogeneous distribution of the fibers must be promoted to form a structural support for the material and enable typical strengthening mechanisms of fiber-reinforced cementitious composites, including crack bridging and crack arresting [28]. In addition, when the WCF content is large, the number of fibrous agglomerates in the AAM matrix increases, acting as weak zones for cracking. ANC-based conditioning of fibers resulted in marked improvement in the flexural performance of AAM composites (blue plot) compared to the respective counterparts loaded with untreated WCF. With respect to the AAM formulations incorporating untreated fiber, the nanoclay treatment led to a strength increment of 19% and 11% in *WCF0.25-ANC* and *WCF0.5-ANC* samples, respectively. For fiber dosages above 0.5 wt.%, the increasing rate was + 9% for both formulations (*WCF0.75-ANC* and *WCF1-ANC* samples). It was also observed that by the addition of 0.25 wt.% of nanoclay-activated WCF, the flexural strength was slightly enhanced compared to plain AAM mortar (*WCF0*). However, the strength decreased with further fiber additions, up to 15%, which is recorded for the *WCF1-ANC* mix. The achieved results suggest that the proposed treatment of fibers with nanoclay benefits the fibers' dispersion and strength performance of the composite up to a specific limit (in this case 0.25 wt.%). When the WCF content is higher, the effect of ANC treatment seems to be ineffective due to the fasciculation mechanisms of the fibers [29,30] and the presence of a growing concentration of residual fibrous clusters that do not undergo deagglomeration following the conditioning.

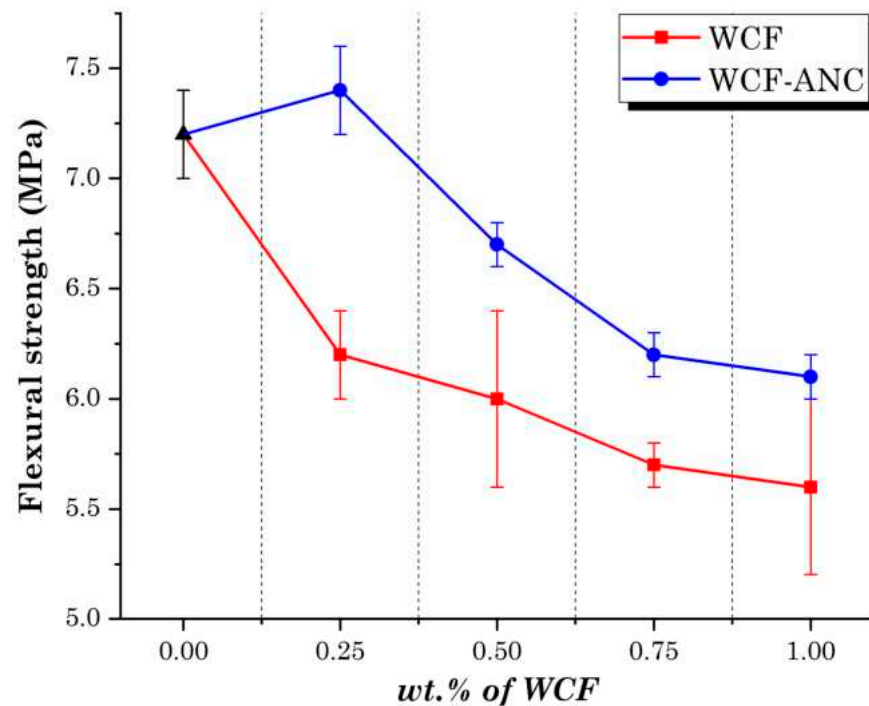


Figure 10. Effect of WCF addition and ANC treatment of fiber on flexural strength of alkali-activated mortars.

Compression strength test results are illustrated in Figure 11. The treatment of fibers with ANC establishes an improvement in mechanical strength compared to the alkali-activated mortars loaded with untreated WCF for concentrations within 0.5 wt.%. However, the effect of nanoclay is confirmed to be progressively more ineffective for higher fiber dosages. As verified for flexural behavior, if the fiber fraction is too high, the defectiveness of the material (fibers agglomeration and clusters) inhibits the dispersing effect of the nanoclay, hindering the improvement of the strength. Regardless of the treatment with ANC, the addition of WCF reduces the compressive strength compared to the simple sample (WCF0). Carbon fibers are high-modulus fibers; therefore, the load-bearing skeleton cannot form in the matrix when fiber dispersion is not optimal. In this case, the enhancement effect on compressive behavior is smaller than the negative effects of the defects caused by the WCF agglomerates [31].

As previously mentioned, the authors studied the addition of the same waste fraction of carbon microfibers in an ordinary cement matrix [13]. The influence of WCF on the mechanical performance of cement-based mortar was completely opposite to the behavior found in the AAM matrix detected in this research. The normalized flexural strength ratio [32], reported in Figure 12, is calculated to elucidate the effect of ANC-treated WCF on the strength performance of AAM and cementitious matrices. For each fiber-added mortar formulation (both cement matrix and AAM), the flexural strength value was divided by the strength of the “control” mortar without WCFs (normalized flexural strength ratio = 1). From the plot below, it appears evident that the WCFs induce a marked improvement in the mechanical characteristics of the cement mortar, and this is also confirmed for high fiber dosage. This would suggest that the dispersion of WCF in the cement paste occurs in a more favorable way than that found in the alkali-activated matrix. Consequently, the action of the ANC is also more efficient in ensuring the correct distribution of the reinforcement in the matrix. One possible explanation for this evidence can be the different rheological properties between the AAM and cement pastes. Criado et al. [33] analyzed and compared the rheology of alkali-activated and Portland cement systems. They observed that the plastic viscosity of AAM is much greater than the cement paste, mainly due to the morphological differences in the particles of the starting materials (angular-shaped cement

particles vs. spherical-shaped FA particles) and the different reaction mechanisms leading to the creation of different hydration products (C-S-H gel short chains in cement system vs. cross-linked aluminosilicate gel in AAM system). Therefore, the higher viscosity of the alkali-activated mixtures hinders the effect of the nanoclay on the declustering and dispersion of the fibers in the matrix. Rheological measurements of the investigated systems can be planned in future research to optimize the fresh-state AAM mix design and achieve adequate rheological properties to ensure superior dispersion of the fibers, boosting their reinforcing effect.

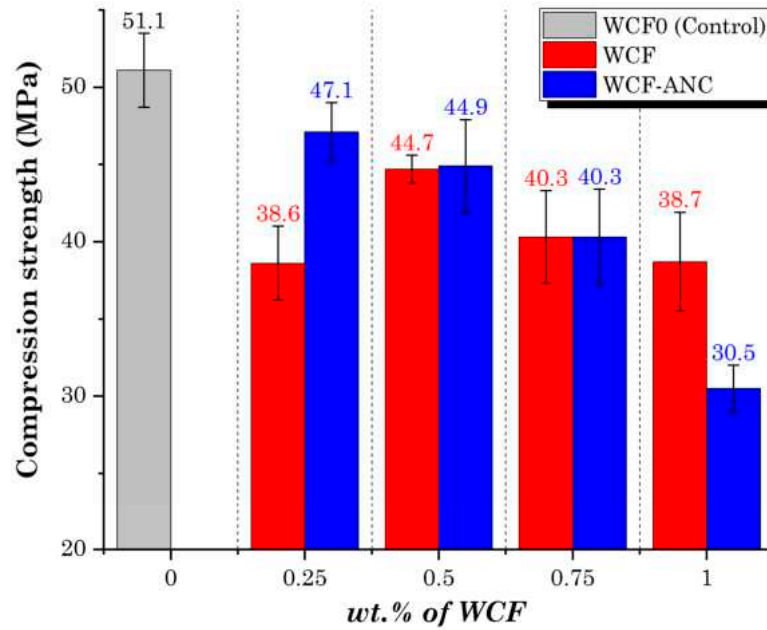


Figure 11. Effect of WCF addition and ANC treatment of fiber on compression strength of alkali activated mortars.

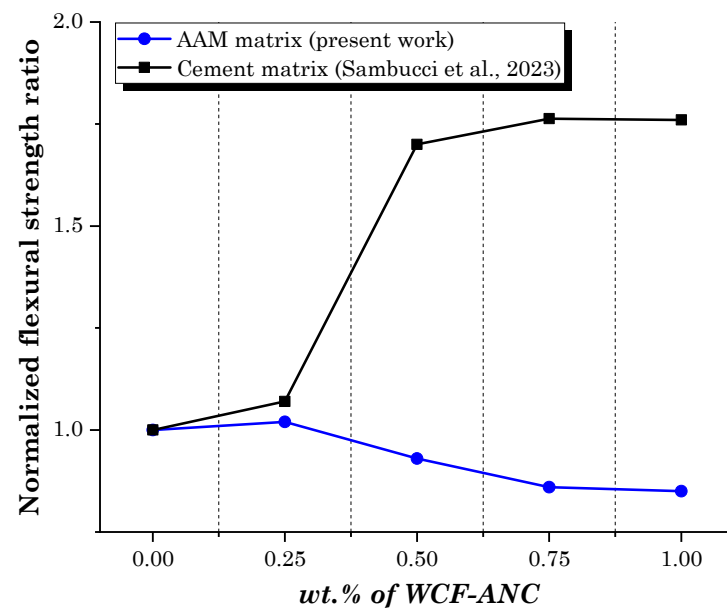


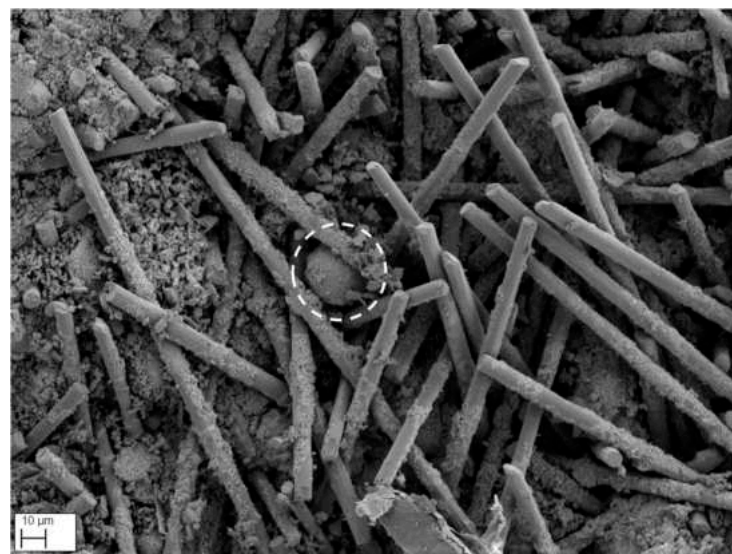
Figure 12. Effect of ANC-treated WCF addition on the flexural behavior of AAM (present work) and cement-based [13] mortars.

3.2.2. SEM Fractography Analysis

SEM micrographs in Figure 13 display the microstructure of alkali-activated mortars incorporating untreated WCF. The lack of adequate dispersibility of fibers brings in the presence of fibrous clusters inside the matrix (Figure 13a). These WCF agglomerates compromise the compactness of the material, causing the formation of voids inside the matrix. Then, under loading, these weak zones tend to induce stress concentrations in the mortar, where premature failure is prone to occur. The effect derived herein agrees with those verified in Ref. [34]. The SEM image in Figure 13b probes the inner microstructure of the fibrous mass. It is noted that the WCF agglomerates trap the aluminosilicate precursors (FA particles) within them (see dotted circle), hindering the potential dissolution with the alkali activator and therefore mitigating their contribution to the proper strength and microstructural development of the AAM matrix. This fact is a further reason to corroborate the significant strength reduction experienced by fiber-reinforced mortars with unconditioned WCF.



(a)



(b)

Figure 13. SEM analysis of alkali-activated mortar with unconditioned WCF (WCF0.5 sample): (a) fibrous agglomerate inside the matrix and (b) detail of the inner microstructure of the WCF cluster. Dotted circle highlights a fly ash particle trapped between the fibers.

Conditioning the WCF permits the investigation of the single-fiber interfacial property with the surrounding alkali-activated matrix thanks to the slightly enhanced dispersion by nanoclay-based treatment. The fractography images in Figure 14 highlight the details of fiber–matrix interaction. Both micrographs display fibers well embedded in the surrounding alkali-activated matrix, denoting that fiber breakage governs the failure of the fiber-reinforced mortar rather than the fiber pull-out. It is known that fiber breakage is the mechanism that occurs when an intimate bond is established between fiber and matrix and is uncommon in concrete materials due to the weak adhesion between fiber and matrix [35]. This evidence would suggest that the nanoclay, in addition to improving the dispersibility of the fibrous clusters, makes the carbon fiber (typically inert towards ceramic–cementitious matrices) chemically more compatible with AAM. The effectiveness of ANC as a surface functionalizing agent was demonstrated by Chougan et al. [36], who increased the compatibility of wheat straw fillers in AAM-based composites, achieving remarkable improvement in strength performance. This effect slightly enhances the flexural behavior of the mortars for low fiber dosage. Once a certain threshold (0.25 wt.% of WCF) is exceeded, the re-agglomeration of the fibers and the presence of multiple residual WCF agglomerates not extricated from the ceramic pre-treatment prevail over the surface functionalization effect of ANC. The deterioration of the mechanical strength compared to the *WCF0* sample is therefore noticeable. Gu et al. [37] observed that carbon fibers tend to agglomerate in FA-GBBS geopolymer composites when the amount exceeds 0.4 wt.%, inducing strength reduction. The authors found that over this threshold, the paste could not flow through the inside of the agglomerated carbon fibers, thus introducing air within the matrix, which forms porosity.

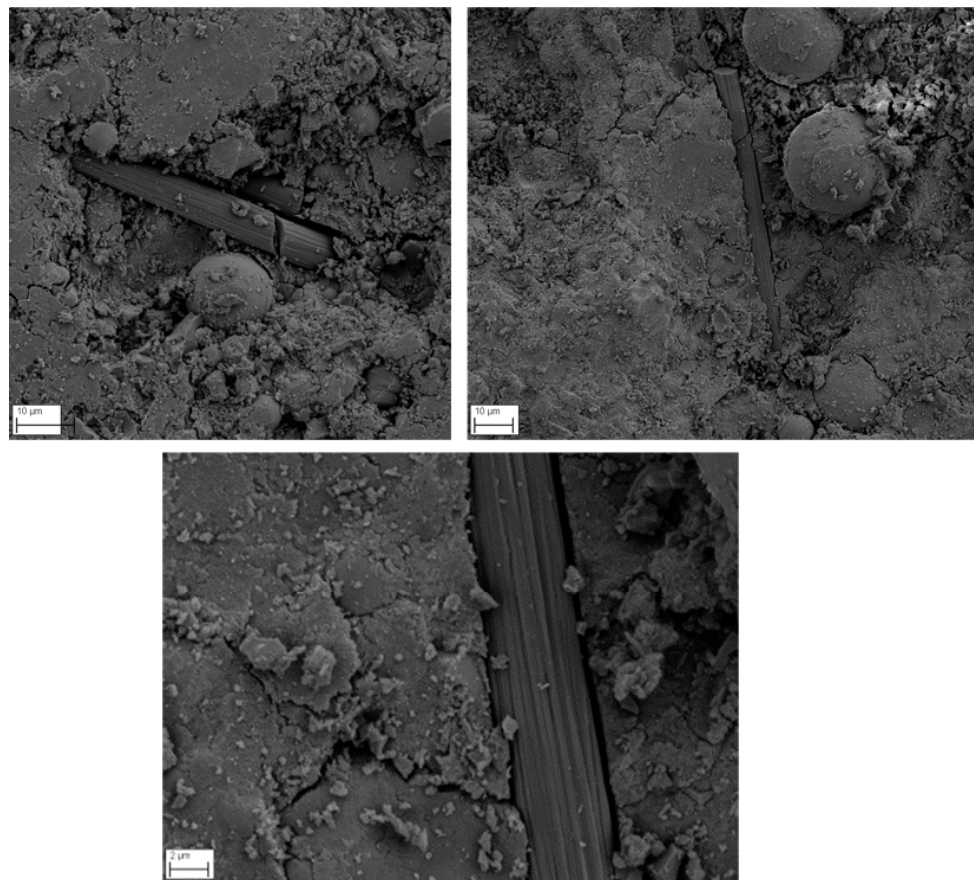


Figure 14. SEM interface analysis between the WCF–ANC and AAM matrix. The micrographs refer to the *WCF0.25-ANC* sample (optimal mix).

4. Conclusions

This study explored the influence of WCFs on the microstructure and mechanical behavior of “one-part” alkali-activated materials. The waste fibers were functionalized with a nanoclay-based surface treatment to attempt improvements in terms of deagglomeration, dispersibility, and compatibility with the AAM matrix. The nanoceramic conditioning was implemented based on a previous work of authors on cement-based mortars to gain comprehensive knowledge about the possibility of using these waste fillers in construction applications. The following concluding remarks can be drawn:

- Further targeted analysis conducted on post-conditioned fibers verified an adequate interaction of the nanoceramic coating with WCFs and a significant increase in hydrophilicity, thus promoting the deagglomeration of the fibrous clusters.
- The mortars produced with ANC-treated WCF showed improvements in mechanical strength compared to those incorporating unconditioned fibers. The maximum increment in flexural strength (+19%) was found in *WCF0.25-ANC*. As the fiber dosage increased, the improving effect was gradually reduced due to the ineffectiveness of the nanoceramic treatment in compensating for fiber declustering.
- Only the formulation with the lowest fiber content (*WCF0.25-ANC*) proved a slight improvement in flexural performance compared to the plain mortar. This result corroborates the above conclusion regarding the difficulty of ensuring a stable integration of the reinforcement for high WCF concentrations.
- From the microstructural analysis, it was clear that the presence of WCF agglomerates, in addition to acting as structural defects, limited the alkaline activation and dissolution of the aluminosilicate precursors, mitigating the proper strength development of the matrix. In this sense, fiber declustering is crucial. Fiber breakage appeared to be the main failure mechanism of the mortars incorporating nanoceramic-functionalized fibers, indicating good fiber–matrix cohesion.

The combination of waste fibers and AAM is undoubtedly an attractive path toward the development of high-performance and green construction materials. However, many investigations still need to be carried out to better understand the main aspects that limit the reinforcing effect of these fibers in alkali-activated matrices. Adjusting the nanoceramic treatment according to the rheology of the AAM mixtures may represent a future research effort stimulated by the successful outputs obtained by implementing these scrap fibers in traditional cementitious systems.

Author Contributions: Conceptualization, M.S., M.C., S.H.G., and M.V.; methodology, M.S., Y.A.A.-N., S.M.N., and M.C.; validation, M.S., Y.A.A.-N., S.M.N., and M.C.; investigation, M.S., Y.A.A.-N., S.M.N., and M.C.; resources, S.H.G. and M.V.; data curation, M.S., S.H.G., and M.V.; writing—original draft preparation, M.S.; writing—review and editing, M.S., Y.A.A.-N., S.H.G., and M.V.; supervision, S.H.G. and M.V.; project administration, S.H.G. and M.V.; funding acquisition, M.S., S.H.G., and M.V. All authors have read and agreed to the published version of the manuscript.

Funding: This research received no external funding.

Institutional Review Board Statement: Not applicable.

Informed Consent Statement: Not applicable.

Data Availability Statement: The data presented in this study are available in this article.

Acknowledgments: This study was carried out within the MICS (Made in Italy—Circular and Sustainable) Extended Partnership and received funding from the European Union Next-GenerationEU (PIANO NAZIONALE DI RIPRESA E RESILIENZA (PNRR)—MISSIONE 4 COMPONENTE 2, INVESTIMENTO 1.3—D.D. 1551.11-10-2022, PE00000004). This manuscript reflects only the authors' views and opinions; neither the European Union nor the European Commission can be considered responsible for them. The authors would like to thank Christian Scopinich (Carbon Task Srl) for providing waste carbon fibers implemented in this study. The authors also appreciate support from Paola Russo and Sofia Ubaldi (Sapienza University of Rome) for running the Fourier-transform

infrared spectroscopy tests. Finally, special thanks to Maria Gabriella Santonicola, Elisa Toto, and Gianluca Ciarleglio (Sapienza University of Rome) for the water contact angle measurements.

Conflicts of Interest: The authors declare no conflicts of interest.

References

- Valente, M.; Sambucci, M.; Chougan, M.; Ghaffar, S.H. Composite alkali-activated materials with waste tire rubber designed for additive manufacturing: An eco-sustainable and energy saving approach. *J. Mater. Res. Technol.* **2023**, *24*, 3098–3117. [\[CrossRef\]](#)
- Eskandarinia, M.; Esmailzade, M.; Aslani, F. Splitting tensile strength of recycled tire steel fiber-reinforced alkali-activated slag concrete designed by Taguchi method. *Struct. Concr.* **2023**, *24*, 3365–3384. [\[CrossRef\]](#)
- Mahmood, A.; Noman, M.T.; Pechočiková, M.; Amor, N.; Petru, M.; Abdelkader, M.; Militký, J.; Sozcu, S.; Hassan, S.Z.U. Geopolymers and Fiber-Reinforced Concrete Composites in Civil Engineering. *Polymers* **2021**, *13*, 2099. [\[CrossRef\]](#) [\[PubMed\]](#)
- de Souza Abreu, F.; Ribeiro, C.C.; da Silva Pinto, J.D.; Nsumbu, T.M.; Buono, V.T.L. Influence of adding discontinuous and dispersed carbon fiber waste on concrete performance. *J. Clean. Prod.* **2020**, *273*, 122920. [\[CrossRef\]](#)
- Xu, J.; Yin, T.; Wang, Y.; Liu, L. Anisotropic electrical and piezoresistive sensing properties of cement-based sensors with aligned carbon fibers. *Cem. Concr. Compos.* **2021**, *116*, 103873. [\[CrossRef\]](#)
- Mechtcherine, V.; Michel, A.; Liebscher, M.; Schneider, K.; Großmann, C. Mineral-impregnated carbon fiber composites as novel reinforcement for concrete construction: Material and automation perspectives. *Autom. Constr.* **2020**, *110*, 103002. [\[CrossRef\]](#)
- Jiang, L.; Ulven, C.A.; Gutschmidt, D.; Anderson, M.; Baló, S.; Lee, M.; Vigness, J. Recycling carbon fiber composites using microwave irradiation: Reinforcement study of the recycled fiber in new composites. *J. Appl. Polym. Sci.* **2015**, *132*. [\[CrossRef\]](#)
- Lamba, N.; Raj, R.; Singh, P. The effects of recycled carbon fibers on the mechanical properties of high-strength concrete and its resilience to impact. *Iran. J. Sci. Technol. Trans. Civ. Eng.* **2023**, 1–23. [\[CrossRef\]](#)
- Patchen, A.; Young, S.; Penumadu, D. An Investigation of Mechanical Properties of Recycled Carbon Fiber Reinforced Ultra-High-Performance Concrete. *Materials* **2023**, *16*, 314. [\[CrossRef\]](#)
- Wang, Y.; Sun, L.; Li, A.; Li, W.; Guo, B. Effect of modified recycled carbon fibers on the conductivity of cement-based materials. *Constr. Build. Mater.* **2024**, *415*, 135033. [\[CrossRef\]](#)
- Li, H.; Liebscher, M.; Yang, J.; Davoodabadi, M.; Li, L.; Du, Y.; Yang, B.; Hempel, S.; Mechtcherine, V. Electrochemical oxidation of recycled carbon fibers for an improved interaction toward alkali-activated composites. *J. Clean. Prod.* **2022**, *368*, 133093. [\[CrossRef\]](#)
- Balea, A.; Fuente, E.; Monte, M.C.; Blanco, A.; Negro, C. Recycled Fibers for Sustainable Hybrid Fiber Cement Based Material: A Review. *Materials* **2021**, *14*, 2408. [\[CrossRef\]](#) [\[PubMed\]](#)
- Sambucci, M.; Valente, M.; Nouri, S.M.; Chougan, M.; Ghaffar, S.H. Enhanced Compatibility of Secondary Waste Carbon Fibers through Surface Activation via Nanoceramic Coating in Fiber-Reinforced Cement Mortars. *Coatings* **2023**, *13*, 1466. [\[CrossRef\]](#)
- Sambucci, M.; Nouri, S.M.; Tayebi, S.T.; Valente, M. Synergic Effect of Recycled Carbon Fibers and Microfibrillated Cellulose Gel for Enhancing the Mechanical Properties of Cement-Based Materials. *Gels* **2023**, *9*, 981. [\[CrossRef\]](#)
- Al-Noaimat, Y.A.; Chougan, M.; Al-kheetan, M.J.; Yio, M.H.; Wong, H.S.; Ghaffar, S.H. Upcycling end-of-life bricks in high-performance one-part alkali-activated materials. *Dev. Built Environ.* **2024**, *16*, 100231. [\[CrossRef\]](#)
- Toto, E.; Laurenzi, S.; Pellegrini, R.C.; Cavallini, E.; Santonicola, M.G. Eco-friendly synthesis of high-performance polyimide materials using bio-based greener solvents: Towards sustainable technologies in space environment. *Mater. Today Sustain.* **2024**, *25*, 100657. [\[CrossRef\]](#)
- Methods of Testing Cement. *Part 1: Determination of Strength*; BS EN 196-1:2016; BSI: London, UK, 2016.
- Jiang, G.; Pickering, S.J. Structure–property relationship of recycled carbon fibres revealed by pyrolysis recycling process. *J. Mater. Sci.* **2016**, *51*, 1949–1958. [\[CrossRef\]](#)
- Zhang, D.; Xu, Y.; Li, X.; Wang, L.; He, X.; Ma, Y.; Zou, D. The Immobilization Effect of Natural Mineral Materials on Cr(VI) Remediation in Water and Soil. *Int. J. Environ. Res. Public Health* **2020**, *17*, 2832. [\[CrossRef\]](#)
- Elbassyoni, S.; Kamoun, E.A.; Taha, T.H.; Rashed, M.A.; ElNozahi, F.A. Effect of Egyptian attapulgitic clay on the properties of PVA-HES–clay nanocomposite hydrogel membranes for wound dressing applications. *Arab. J. Sci. Eng.* **2020**, *45*, 4737–4749. [\[CrossRef\]](#)
- Chung, D.D. Dispersion of short fibers in cement. *J. Mater. Civ. Eng.* **2005**, *17*, 379–383. [\[CrossRef\]](#)
- Ranjbar, N.; Talebian, S.; Mehrali, M.; Kuenzel, C.; Metselaar, H.S.C.; Jumaat, M.Z. Mechanisms of interfacial bond in steel and polypropylene fiber reinforced geopolymer composites. *Compos. Sci. Technol.* **2016**, *122*, 73–81. [\[CrossRef\]](#)
- Diblíková, L.; Mašek, Z.; Král, M. The effect of carbon fiber plasma treatment on the wettability and interlaminar shear strength of geopolymer composite. *J. Aust. Ceram. Soc.* **2019**, *55*, 1139–1145. [\[CrossRef\]](#)
- Zhang, R.; Li, F.; Zhou, S.; Hou, Y. Carbon nanofiber dispersion in alkali solution and its reinforcement of alkali-activated volcanic ash-based geopolymers. *J. Clean. Prod.* **2023**, *405*, 137021. [\[CrossRef\]](#)
- Lindström, T.; Banke, K.; Larsson, T.; Glad-Nordmark, G.; Boldizar, A. Nanoclay plating of cellulosic fiber surfaces. *J. Appl. Polym. Sci.* **2008**, *108*, 887–891. [\[CrossRef\]](#)
- Wang, Y.; Jiang, Y.; Pan, T.; Yin, K. The Synergistic Effect of Ester-Ether Copolymerization Thixo-Tropic Superplasticizer and Nano-Clay on the Buildability of 3D Printable Cementitious Materials. *Materials* **2021**, *14*, 4622. [\[CrossRef\]](#) [\[PubMed\]](#)

27. Zheng, H.; Li, J.; Bian, D.; Ni, Z.; Qian, S.; Zhao, Y. Improving the Tribological Performance of Phosphate-Bonded Coatings Reinforced by Carbon Fiber/Graphene Oxide. *ACS Appl. Nano Mater.* **2023**, *6*, 13374–13384. [[CrossRef](#)]
28. Zhang, P.; Zhao, Y.N.; Liu, C.H.; Wang, P.; Zhang, T.H. Combined effect of nano-SiO₂ particles and steel fibers on flexural properties of concrete composite containing fly ash. *Sci. Eng. Compos. Mater.* **2014**, *21*, 597–605. [[CrossRef](#)]
29. Wang, C.; Li, K.Z.; Li, H.J.; Jiao, G.S.; Lu, J.; Hou, D.S. Effect of carbon fiber dispersion on the mechanical properties of carbon fiber-reinforced cement-based composites. *Mater. Sci. Eng. A* **2008**, *487*, 52–57. [[CrossRef](#)]
30. Akbar, A.; Kodur, V.K.R.; Liew, K.M. Microstructural changes and mechanical performance of cement composites reinforced with recycled carbon fibers. *Cem. Concr. Compos.* **2021**, *121*, 104069. [[CrossRef](#)]
31. Wang, D.; Ju, Y.; Shen, H.; Xu, L. Mechanical properties of high performance concrete reinforced with basalt fiber and polypropylene fiber. *Constr. Build. Mater.* **2019**, *197*, 464–473. [[CrossRef](#)]
32. Cui, Y.; Hao, H.; Li, J.; Chen, W. Effect of adding methylcellulose on mechanical and vibration properties of geopolymer paste and hybrid fiber-reinforced geopolymer composite. *J. Mater. Civ. Eng.* **2020**, *32*, 04020166. [[CrossRef](#)]
33. Criado, M.; Palomo, A.; Fernández-Jiménez, A.; Banfill, P.F.G. Alkali activated fly ash: Effect of admixtures on paste rheology. *Rheol. Acta* **2009**, *48*, 447–455. [[CrossRef](#)]
34. Li, J.; Wang, B.; Zhang, P.; Wang, Z.; Wang, M. Parametric Study on Mechanical Properties of Basalt Fiber-Reinforced Pea Gravel Concrete. *Buildings* **2024**, *14*, 380. [[CrossRef](#)]
35. Deng, Y.; Zhang, Z.; Shi, C.; Wu, Z.; Zhang, C. Steel fiber–matrix interfacial bond in ultra-high performance concrete: A review. *Engineering* **2023**, *22*, 215–232. [[CrossRef](#)]
36. Chougan, M.; Ghaffar, S.H.; Sikora, P.; Mijowska, E.; Kukułka, W.; Stephan, D. Boosting Portland cement-free composite performance via alkali-activation and reinforcement with pre-treated functionalised wheat straw. *Ind. Crops Prod.* **2022**, *178*, 114648. [[CrossRef](#)]
37. Gu, G.; Pei, Y.; Ma, T.; Chen, F.; Zhang, J.; Xu, F. Role of carbon fiber in the electrothermal behavior and geopolymerization process of carbon fiber-reinforced FA-GBFS geopolymer composite. *Constr. Build. Mater.* **2023**, *369*, 130597. [[CrossRef](#)]

Disclaimer/Publisher’s Note: The statements, opinions and data contained in all publications are solely those of the individual author(s) and contributor(s) and not of MDPI and/or the editor(s). MDPI and/or the editor(s) disclaim responsibility for any injury to people or property resulting from any ideas, methods, instructions or products referred to in the content.